Convective Diffusion in Porous Membranes with Adsorbed Charges

Anna-Kaisa Kontturi, Kyösti Kontturi,* Salvador Mafé,† José A. Manzanares,† Pasi Niinikoski, and Mikko Vuoristo

Laboratory of Physical Chemistry and Electrochemistry, Helsinki University of Technology, SF-02150 Espoo 15, Finland

Received August 25, 1993. In Final Form: November 22, 1993®

We have studied experimentally the effects that the charge adsorbed on the membrane pore walls exerts on the convective diffusion through a porous membrane. The plot of the logarithm of the bulk concentration ratio vs convective flow through the membrane is usually employed to determine the membrane parameter A/L (effective membrane area/membrane thickness). It is shown that the deviations from the linear behavior of this plot give us information on the adsorbed charge concentration. A simple model based on the Nernst–Planck equation for the ion fluxes and the Navier–Stokes equation for the pore fluid velocity has proved to be useful for the understanding of the experimental trends observed over a range of membrane pore radius and electrolyte concentration. Our study can be seen as an independent confirmation of a rather general result: ion adsorption to the pore walls of inert, porous membranes can significantly affect the transport phenomena, especially in the limit of low electrolyte concentration.

Introduction

Convective diffusion processes in porous membranes have been extensively studied in connection with new separation methods, such as continuous convective electrophoresis or countercurrent electrolysis (see ref 1 and references therein). These processes have also been utilized in the determination of the diffusion coefficients and the effective charge numbers of a polydisperse polyelectrolyte.[2-5] In all of these studies the porous membrane was considered noncharged. However, the important effects caused by the adsorption of ions on the surface of the polymer membrane matrix have recently been emphasized.[6-9] These adsorbed charges should be included in the model when their effect is great enough so as to influence the transport process.

The measurements considered here concern the membrane parameter A/L (effective membrane area/membrane thickness). This is a key parameter in many physical situations[10,11] and must be determined in a separate measurement, e.g., by plotting the logarithm of the bulk concentration ratio vs convective flow through the membrane. However, we will see here that the charges adsorbed on the walls of the membrane pores can cause important effects on this determination. The main objective of the paper is to study these effects, and give a simple theory to explain them. In particular, we are interested in showing how charged pores (due to ion adsorption) can modify significantly the classical flow equation for convective diffusion in porous media usually employed for determining the membrane parameter A/L. As far as we know, no systematic study of this particular relationship has been previously presented for the experimental conditions considered here. Note that our problem involves the simultaneous gradients of *three* physical magnitudes (concentration, pressure, and electric potential) through the membrane. Therefore, the interpretation of the experimental results and the modeling of the transport problem are considerably difficult. Analytic and semianalytic models[12] have usually been concerned with only *two* of the above gradients, and cannot then be applied to our problem. (This is also the case in the experimental studies; see, e.g., refs 6–10.) Although excellent work concerning the *numerical simulation* of membrane systems under general experimental conditions has recently appeared,[9] we felt that giving *approximate analytical* solutions to some practical problems can be of interest to the experimentalist, at least for the particular situation dealt with here.

The structure of the paper is as follows. First, we state the experimental convective diffusion phenomenon analyzed. Then, we present the results obtained, and finally, we give a theoretical approach that can explain all the experimental trends observed.

Experimental Section

Apparatus. The membrane cell made of Perspex glass is described in Figure 1. The exposed membrane area was a circle of ca. 1 cm^2. The volume of the α-compartment was small (3.4 mL) compared to that of the β-compartment (1000 mL). The

† Permanent address: Department of Thermodynamics, Faculty of Physics, University of Valencia, E-46100 Burjasot, Spain.

® Abstract published in *Advance ACS Abstracts*, February 1, 1994.

(1) Kontturi, A. K.; Kontturi, K.; Savonen, A.; Vuoristo, M.; Schiffrin, D. J. *J. Chem. Soc., Faraday Trans.* **1993**, *89*, 99.

(2) Kontturi, A. K.; Kontturi, K. *J. Colloid Interface Sci.* **1987**, *120*, 256.

(3) Kontturi, A. K.; Kontturi, K. *J. Colloid Interface Sci.* **1988**, *124*, 328.

(4) Kontturi, A. K.; Kontturi, K.; Niinikoski, P. *J. Chem. Soc., Faraday Trans.* **1990**, *86*, 3097.

(5) Kontturi, A. K.; Kontturi, K.; Niinikoski, P. *J. Chem. Soc., Faraday Trans.* **1991**, *87*, 1779.

(6) Westermann-Clark, G. B.; Anderson, J. L. *J. Electrochem. Soc.* **1983**, *130*, 839. Mafé, S.; Manzanares, J. A.; Pellicer, J. *J. Membr. Sci.* **1990**, *51*, 161. Manzanares, J. A.; Mafé, S.; Ramírez, P. *J. Non-Equilib. Thermodyn.* **1991**, *16*, 255.

(7) Hernández, A.; Ibáñez, J. A.; Martínez, L.; Tejerina, A. F. *Sep. Sci. Technol.* **1987**, *22*, 1235.

(8) Takagi, R.; Nakagaki, M. *J. Membr. Sci.* **1990**, *53*, 19. Aguilella, V. M.; Manzanares, J. A.; Pellicer, J. *Langmuir* **1993**, *9*, 550.

(9) Pintauro, P. N.; Verbrugge, M. W. *J. Membr. Sci.* **1989**, *44*, 197. Verbrugge, M. W.; Pintauro, P. N. Transport models for ion-exchange membranes. In *Modern Aspects of Electrochemistry*; Conway, B. E., Bockris, J. O., White, R. E., Eds.; 1989; Vol. 19, p 1. Guzmán-García, A. G.; Pintauro, P. N.; Verbrugge, M. W.; Hill, R. F. *AIChE J.* **1990**, *36*, 1061.

(10) Kontturi, K.; Savonen, A.; Vuoristo, M. *Acta Chem. Scand.*, in press.

(11) Johnson, K. A.; Westermann-Clark, G. B.; Shah, D. O. *Langmuir* **1989**, *5*, 932.

(12) Rice, C. L.; Whitehead, R. *J. Phys. Chem.* **1965**, *69*, 4017. Newman, J. *Electrochemical Systems*; Prentice-Hall: New York, 1973; p 193. Levine, S.; Marriot, J. R.; Neale, G.; Epstein, N. *J. Colloid Interface Sci.* **1975**, *52*, 136.

0743-7463/94/2410-0949$04.50/0

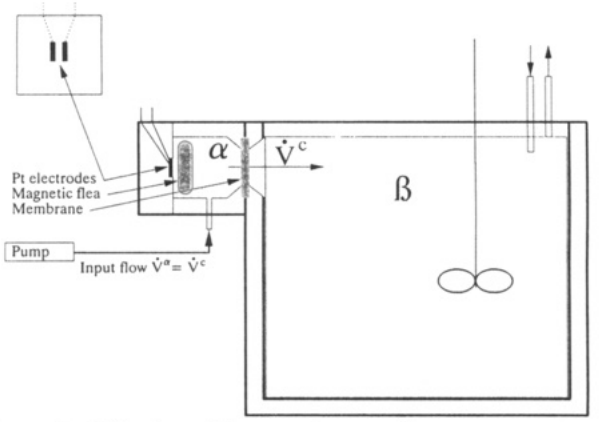

Figure 1. Side view of the membrane cell.

convection flow $\dot{V}^\alpha$ was controlled by a syringe pump (Sage Instruments Model 341B). The temperature was maintained at 25 °C by circulating the input flow through a thermostated bath (Haake D8) and using a heat exchanger in the β-compartment. The two Pt electrodes in the α-compartment were connected to a Philips PW9527 conductivity meter. The conductivity of the α-compartment was monitored continuously by an x–t recorder (BBC Goerz Metrawatt SE120) connected to the analog output of the conductivity meter. A pressure sensor (Sen Sym SCX01DNC) was installed to the input flow tube to monitor the pressure difference developed across the membrane.

Note that the particular cell design shown in Figure 1 permits the condition of zero salt flux to be achieved: a convective flow is imposed in opposition to a concentration gradient. Initially, the concentration gradient dominates over the convective flow, but when the steady state is finally reached, the two terms just cancel each other to give a zero salt flux.

Materials. Two types of Millipore filters were used as porous membranes: Durapore VVLP and MF-Millipore with mean pore sizes of 0.1 and 0.22 μm, respectively. Sodium chloride and potassium chloride solutions were made by using pro analysis grade products (Merck) and milli-Q water (Waters).

Measurements. The porous membrane was soaked in milli-Q water for at least 48 h before use. Once the cell was assembled, the α-compartment was carefully filled by feeding milli-Q water using the syringe pump. The β-compartment was then filled by 0.01 M sodium chloride, 0.1 M sodium chloride, or 0.01 M potassium chloride already thermostated to 25 °C. The experiment was started by selecting the pumping rate and by starting the monitoring of the conductivity and of the pressure difference. The system was in a steady state when the conductivity of the α-compartment had reached a constant value. This value was also used to calculate the steady-state concentration of the α-side. The next pumping rate was then selected. The pumping rates varied from 8.4 to 0.34 mL/h. Fresh solutions were changed to the β-compartment twice a day. For each combination of membrane and β-side solution a new porous membrane was prepared.

The conductivity measurement was calibrated after each experiment by feeding standard solutions of sodium chloride or potassium chloride to the α-compartment. The β-compartment was empty in these experiments. The standard solutions were made by using the same stock of milli-Q water that had been used in the actual experiments.

Durapore VVLP was used with the following β-side solutions: 0.01 M sodium chloride, 0.1 M sodium chloride, and 0.01 M potassium chloride. MF-Millipore was used with 0.01 M sodium chloride in the β-side. In addition, a Durapore VVLP with a very small scratch was used in order to demonstrate the results in the absence of small pores.

Results

The experimental results are shown in Table 1 in the form of the logarithm of the concentration ratio, $\ln(c^\beta/c^\alpha)$, as a function of convective flow through the membrane, $\dot{V}^c$. All data correspond to the Durapore membrane

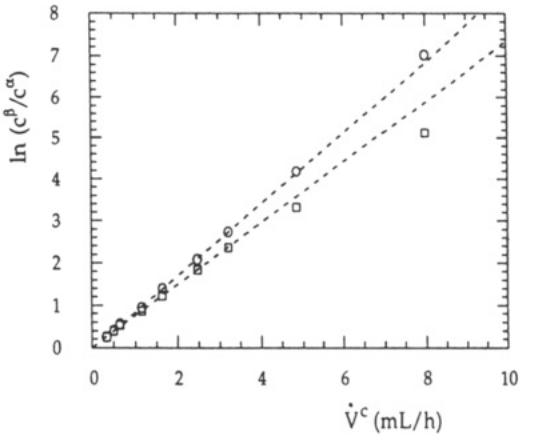

Figure 2. Logarithm of the concentration ratio as a function of convective flow: (s) 0.01 M NaCl, scratch in the membrane (○), and (a) 0.01 M NaCl (□). The regression (dashed) line has been calculated using the points below 2 mL/h.

Table 1. Logarithm of the Concentration Ratio as a Function of Convective Flow for the following Cases: (s) 0.01 M NaCl, Durapore Membrane with a Small Scratch, (a) 0.01 M NaCl, Durapore Membrane; (b) 0.1 M NaCl, Durapore Membrane; (c) 0.01 M KCl, Durapore Membrane, and (d) 0.01 M NaCl, MF-Millipore Membrane

	$\ln(c^\beta/c^\alpha)$				
$\dot{V}^c$ (mL/h)	s	a	b	c	d
0.34	0.253	0.248			
0.51	0.405	0.397	0.412	0.451	0.328
0.65	0.559	0.534	0.533	0.462	0.426
1.16	0.942	0.865	0.962	0.796	0.753
1.64	1.389	1.221	1.386	1.149	1.106
2.48	2.083	1.833	2.071	1.625	1.514
3.21	2.736	2.358	2.690	2.129	2.112
4.85	4.173	3.321	3.777	3.172	3.060
7.98	7.018	5.129	5.956	5.022	4.878

(except for those in case d, which were obtained with the MF-Millipore membrane). The results presented show the effects of changing the membrane pore radius (see cases s, a, and d), the concentration (cases a and b), and the electrolyte system (cases a and c) on the observed phenomena. It can readily be shown that application of the Nernst–Planck equations for the one-dimensional ion transport through the membrane together with the electroneutrality condition would lead to the following well-known theoretical relationship between $\dot{V}^c$ and $\ln(c^\beta/c^\alpha)$:

$$\ln \frac{c^\beta}{c^\alpha} = \frac{\dot{V}^c L}{A D_s} \tag{1a}$$

where L, A, and D_s are, respectively, the membrane thickness, the membrane effective area, and the salt diffusion coefficient. Equation 1a can be obtained by adding the two Nernst–Planck flux equations, and applying the zero ion flux conditions. It predicts a *linear* relationship between $\dot{V}^c$ and $\ln(c^\beta/c^\alpha)$. However, all the experimental results in Table 1 deviate from this linear behavior for small enough values of c^α, except for those corresponding to case s (scratch in the membrane). This effect is shown in Figure 2, where we have considered only cases s and a for the sake of clarity. Indeed, we see that only the results corresponding to the presence of a scratch in the membrane are well described by eq 1a through the whole c^α range.

The deviations from linearity shown in Figure 2 prompted us to look for possible *systematic* errors in the experiments. Since the imposed volume flows were only of a few milliliters per hour, the first hypothesis we

considered and discarded was the existence of leaks in the apparatus. Later, we analyzed the possibility of systematic deviations from the initial concentration in the β-compartment, c^β, during the experiment. However, these were found to be very unlikely to occur, since the volume of this compartment was several orders of magnitude larger than that of the α-compartment and the volume flows were very small. Explanations based on swelling effects were also ruled out, since these effects were not high enough to account for the deviations observed.

A more reasonable approach was based on the existence of diffusion boundary layers (DBLs) with convection-dependent thickness δ. Indeed, the apparatus (see Figure 1) was not specifically designed to minimize the thickness of these layers. Let us study this question in detail. Considering the one-dimensional ion transport through the whole membrane system (i.e., the membrane and the two DBLs), eq 1a can be generalized to

$$\ln \frac{c^\beta}{c^\alpha} = \frac{\dot{V}^c}{A}\left(\frac{L}{D_s} + \frac{2\delta}{D_s^b}\right) = \frac{\dot{V}^c}{A}\left(\frac{L}{D_s} + \frac{2\delta_0}{D_s^b}\right)(1-\epsilon)$$

$$\epsilon \equiv \frac{2\Delta\delta/D_s^b}{(L/D_s) + (2\delta_0/D_s^b)} \tag{1b}$$

where D_s^b is the salt diffusion coefficient in the DBLs, and δ_0 and $\Delta\delta$ are the DBL thickness at $\dot{V}^c = 0$ and its absolute decrease at a given value of $\dot{V}^c$, $\Delta\delta = \delta_0 - \delta(\dot{V}^c)$, respectively. Parameter ϵ in eq 1b accounts for the deviations from the linear behavior shown in Figure 2 through the imposed convective flow $\dot{V}^c$. Equation 1b can now be fitted to the experimental points in Figure 2 (curve a) in order to find out if the resulting reductions in the DBL thickness, $\Delta\delta$, are reasonable. This procedure gives the values $[(L/D_s) + (2\delta_0/D_s^b)]/A = 0.75$ h/mL and $\epsilon = 0.15$.

Now, if we assume $D_s^b/D_s = 10$ (note that diffusion through the membrane is usually slower than diffusion in the bulk solution), the following reductions in δ are obtained from eq 1b: $\Delta\delta/\delta_0 \approx 20\%$ when $L = 0.1\delta_0$ and $\Delta\delta/\delta_0 \approx 90\%$ when $L = \delta_0$. (These figures correspond to the maximum values of the convective flow in Figure 2.) Absurd reductions ($\Delta\delta/\delta_0 > 100\%$) are obtained when the DBL thickness is smaller than the membrane thickness, $L > \delta_0$. Although the above results become less dramatic when $D_s^b/D_s \gtrsim 1$, it seems rather unlikely that a 2-fold change in $\dot{V}^c$ (see Figure 2, case a) could result in such significant reductions in δ. Therefore, although our estimations did not discard definitively an explanation based on the existence of DBLs, we felt that other alternative approaches should be attempted. In particular, the possibility that the charges adsorbed on the pore walls could cause important effects on the convective diffusion through the membrane at low enough values of c^α was considered. We address this question in the next section.

Theoretical Approach

We present now a physical model for describing the behavior of the $\ln(c^\beta/c^\alpha)$ vs $\dot{V}^c$ curves in Table 1 and Figure 2. Although we have derived the exact equations describing the problem, we have finally resorted to a rather simple model. Despite its simplicity, this model can explain the experimental trends observed.

The membrane is simulated by a bank of parallel cylindrical pores (see ref 9 and references therein). The membranes employed do not have a significant concentration of intrinsically ionizable groups, and the negative charge experimentally observed[10] is assumed to be due to the adsorption of chloride ions on the surface of the pores. In the concentration range where the deviations from the linear behavior in the $\ln(c^\beta/c^\alpha)$ vs $\dot{V}^c$ curves occur ($c^\alpha \approx 0.1$ mM) a typical Debye length is $\lambda = (\epsilon RT/F^2c^\alpha)^{1/2} \approx 0.03$ μm, which can be compared with the pore radius $r_0 = 0.05$ μm. Therefore, the electric double layer invades almost all the pore section, and the co-ion is virtually excluded from the pore. Note that this exclusion effect should not appear for large enough values of c^α ($c^\alpha \approx 1$–10 mM), since in this limit $r_0 \gg \lambda$. Accordingly, we see that a one-dimensional model neglecting charge effects at the pore wall would be justified only in the above limit.

In order to arrive at theoretical expressions which can be compared with the experiments, a number of approximations should be made. Bearing in mind the above discussion, a charged capillary tube model based on the idea of total co-ion exclusion should be employed.[6,10] Also, we will introduce the Nernst–Planck equation[13] for the ion flux. Since the experimental conditions considered lead to zero ion flux, the Nernst–Planck equation in the axial direction for the counterion (the positive ion here) is

$$0 = \int_0^{r_0} J(r) 2\pi r\, dr = -D\int_0^{r_0} \frac{\partial c(r,x)}{\partial x} 2\pi r\, dr - D\frac{F}{RT}\int_0^{r_0} c(r,x)\frac{\partial \phi(r,x)}{\partial x} 2\pi r\, dr + \int_0^{r_0} c(r,x)\, v(r) 2\pi r\, dr \tag{2}$$

where D, c, and J are the diffusion coefficient, the molar concentration, and the axial flux of the positive ion, respectively. Also, ϕ is the local electric potential, and v is the convection (pore fluid velocity). Variables x and r stand for the axial position across the membranes (extending from $x = 0$ to $x = L$) and the radial position in the pore section (extending from $r = 0$ to $r = r_0$). Constants F, R, and T have their usual meaning.

Concentration and electric potential are related through the Poisson equation,[9] which can be written for the complete co-ion exclusion case in the form

$$\Delta\phi(r,x) = -\frac{\rho(r,x)}{\epsilon} = -\frac{F}{\epsilon} c(r,x) \tag{3}$$

where Δ represents the Laplacian operator and ρ is the local charge density. For mathematical convenience, ϕ is usually split into two terms:[6]

$$\phi(r,x) = \varphi(r,x) + V(x) \tag{4}$$

where $V(x)$ is considered to be a linear function of the axial coordinate. Taking into account that there is no ion flux in the radial direction, $c(r,x)$ can be written as[6]

$$c(r,x) = C(x)\exp[-(F/RT)\varphi(r,x)] \tag{5}$$

Finally, the Navier–Stokes equation[6,9]

$$\eta\Delta\vec{v}(r) = \vec{\nabla}p(r,x) + \rho(r,x)\vec{\nabla}\phi(r,x) \tag{6}$$

relates the pore fluid velocity $\vec{v} = (v_r v_\theta v_x) = (0,0,v)$ to the pressure (p) and electric potential gradients. In eq 6, η stands for the dynamic viscosity. The simultaneous solution of eqs 2, 3, and 6 poses a formidable problem (even for the limiting case of co-ion exclusion considered here) when a *concentration* gradient coexists simultaneously with *pressure* and *electric potential* gradients, as is our case. On the other hand, the effort of obtaining an exact (numerical) solution of the problem is not probably justified here, since we are just seeking a reasonable explanation for the behavior of the $\ln(c^\beta/c^\alpha)$ vs $\dot{V}^c$

(13) Buck, R. P. *J. Membr. Sci.* **1984**, *17*, 1.

experimental curves rather than trying to develop a rigorous theory for convective diffusion phenomena in charged capillary tubes.[9] Therefore, we will derive first the formal solution of the equations, and then introduce a number of approximations relevant to our problem. This procedure will lead finally to a very simple equation which is able to describe the experimental trends observed.

By using eqs 2 and 6 with the expressions for $\phi(r,x)$ and $c(r,x)$ given in eqs 4 and 5, the following formal solution for the convection profile in the pore can be obtained:

$$v(r) = -\frac{1}{4\eta}\frac{dp(0,x)}{dx}(r_0^2 - r^2) + \frac{RT}{4\eta}\frac{dC(x)}{dx}(r_0^2 - r^2) - \frac{RTC(x)}{2\pi D\eta}\frac{\int_0^{r_0} e^{-F\varphi/RT} v 2\pi r'\, dr'}{\int_0^{r_0} e^{-F\varphi/RT} 2\pi r'\, dr'}\int_r^{r_0}\left(\int_0^{r'} e^{-F\varphi/RT} 2\pi r''\, dr''\right)\frac{dr'}{r'} \quad (7)$$

where the boundary conditions $v(r_0) = 0$ and $(dv/dr)(0) = 0$ have been imposed. In obtaining eq 7, we have considered separately the axial and radial components of eq 6:

$$\eta\frac{1}{r}\frac{d}{dr}\left(r\frac{dv}{dr}\right) = \frac{\partial p}{\partial x} + FCe^{-F\varphi/RT}\left(\frac{\partial\varphi}{\partial x} + \frac{dV}{dx}\right) \quad (8a)$$

$$0 = \frac{\partial p}{\partial r} + FCe^{-F\varphi/RT}\frac{\partial\varphi}{\partial r} \quad (8b)$$

respectively. The electric potential $\varphi(r,x)$ in eq 7 must be obtained from the Poisson equation (3) in the form

$$\frac{1}{r}\frac{\partial}{\partial r}\left(r\frac{\partial\varphi}{\partial r}\right) + \frac{\partial^2\varphi}{\partial x^2} = -\frac{F}{\epsilon}Ce^{-F\varphi/RT} \quad (9)$$

Instead of performing the numerical integration of the equation system, we will derive an intuitive, simple solution to the problem that will prove to be useful for our purposes in this study. Let us consider first eq 7. If $\varphi(r,x)$ does not change very much with r (a situation very common when the condition of total co-ion exclusion holds[14]), then $e^{-F\varphi/RT}$ is nearly constant and eq 7 leads to

$$v(r) \approx v(0)[1 - (r/r_0)^2] \quad (10)$$

where $v(0)$ can be obtained from the comparison of eqs 7 and 10 in the limit considered. We can introduce the profile $v(r)$ given in eq 10 into eq 8a, and solve for $Fc(\partial\phi/\partial x)$. Further substitution of $Fc(\partial\phi/\partial x)$ into eq 2 leads to

$$\frac{d}{dx}\left(\int_0^{r_0} c 2\pi r\, dr\right) - \frac{1}{RT}\int_0^{r_0}\left(\frac{4\eta v(0)}{r_0^2} + \frac{\partial p}{\partial x}\right)2\pi r\, dr - \frac{1}{D}\int_0^{r_0} cv 2\pi r\, dr = 0 \quad (11)$$

The first integral in eq 11 is the result of averaging the local concentration $c(r,x)$ over the pore cross section. We will write its value as $\bar{c}A_{pore}$, where A_{pore} is the pore area. According to this interpretation, the third integral can be written as

$$\int_0^{r_0} cv 2\pi r\, dr = \overline{cv}A_{pore} \approx \bar{c}\bar{v}A_{pore} \equiv \bar{c}\dot{V}^c_{pore} \quad (12)$$

where

$$\dot{V}^c_{pore} \equiv \int_0^{r_0} v 2\pi r\, dr \quad (13)$$

is the volume flow through the pore. The approximation in eq 12 is consistent with the assumption previously introduced for φ in order to obtain eq 10 from eq 7.

Consider now the second integral in eq 11. From eqs 10 and 13, it can be readily shown that $v(0) = 2\dot{V}^c_{pore}A_{pore}$. Substituting all the above results into eq 11, we have

$$\frac{d\bar{c}}{dx} - \frac{1}{RT}\left(\frac{8\eta\dot{V}^c_{pore}}{r_0^2 A_{pore}} + \frac{dp}{dx}\right) - \frac{\bar{c}\dot{V}^c_{pore}}{DA_{pore}} = 0 \quad (14)$$

where we have assumed that the pressure changes only in the axial direction. Now, if we divide every term in eq 14 by $\bar{c}$, and refer the ratio $\dot{V}^c_{pore}/A_{pore}$ to the whole membrane rather than to the pore, then we obtain

$$\frac{d\ln\bar{c}}{dx} + \frac{1}{RT\bar{c}}\left(-\frac{8\eta\dot{V}^c}{r_0^2 A} - \frac{dp}{dx}\right) - \frac{\dot{V}^c}{DA} = 0 \quad (15)$$

where A is the effective membrane area and $\dot{V}^c$ is the total volume flow through the membrane ($\dot{V}^c/A = N_{pores}\dot{V}^c_{pore}/N_{pores}A_{pore} = \dot{V}^c_{pore}/A_{pore}$, N_{pores} being the number of pores in the membrane). Consider next the two terms within the parentheses in eq 15. The first one is negative and arises from the retarding viscous force which acts on a given volume of the pore fluid. The second one ($-dp/dx$) is positive (see the experimental setup) and pushes the fluid toward the right bulk solution. On the other hand, it is clear that the axial component of the electric field ($-\partial\phi/\partial x$) must produce a negative force, since the pressure gradient applied initially made the positively charged pore fluid move toward the right bulk solution (see the experimental setup). Now, for the pore fluid to move at constant speed, all the above three forces must add to give a zero total force (see eq 6). Since the three forces have similar orders of magnitude, eq 6 imposes that

$$-\frac{dp}{dx} \gtrsim \frac{8\eta\dot{V}^c}{r_0^2 A} \quad (16)$$

We conclude that the eq 15 can be written in the form

$$\frac{d\ln\bar{c}}{dx} + \gamma\frac{1}{RT\bar{c}}\frac{8\eta\dot{V}^c}{r_0^2 A} - \frac{\dot{V}^c}{DA} = 0 \quad (17)$$

where, according to the above reasoning, $\gamma \lesssim 1$.

We proceed now to integrate eq 17 along the membrane. This yields

$$\ln\frac{\bar{c}(L)}{\bar{c}(0)} = \frac{\dot{V}^c L}{AD}\left[1 - \frac{8\gamma\eta D}{RTr_0^2 L}\int_0^L\frac{dx}{\bar{c}}\right] \approx \frac{\dot{V}^c L}{AD}\left[1 - \frac{8\gamma\eta D}{RTr_0^2\bar{c}(0)}\right] \quad (18)$$

where the interfacial concentrations are given by Donnan equilibrium[15] relationships at the membrane interfaces, $\bar{c}(0) = (X(0)/2) + [(X(0)/2)^2 + (c^\alpha)^2]^{1/2}$ and $\bar{c}(L) = (X(L)/2) + [(X(L)/2)^2 + (c^\beta)^2]^{1/2}$ (X is the adsorbed charge concentration). In eq 18 we have used the assumption $\bar{c}(x) \approx \bar{c}(0)$ when evaluating the integral. At first, it might seem that $\bar{c}(x)$ cannot be constant along the membrane because of the difference in the two bulk solution concentrations. However, assume $\bar{c}(x) \approx \bar{c}(0)$ remains valid over most of the membrane thickness due to the large convective flow superimposed to the concentration gradient,[16] and only breaks down in the vicinity of $x = L$ where $\bar{c}$ increases sharply to reach a value close to c^β (see Figures 1 and 2 and Table 1). Indeed, note that the Peclet

(14) Cwirko, E. H.; Carbonell, G. *J. Colloid Interface Sci.* **1989**, *129*, 513.

(15) Helfferich, F. *Ion exchange*; MacGraw-Hill: New York, 1962.

(16) Ekman, A.; Forsell, P.; Kontturi, K.; Sundholm, G. *J. Membr. Sci.* **1982**, *11*, 65.

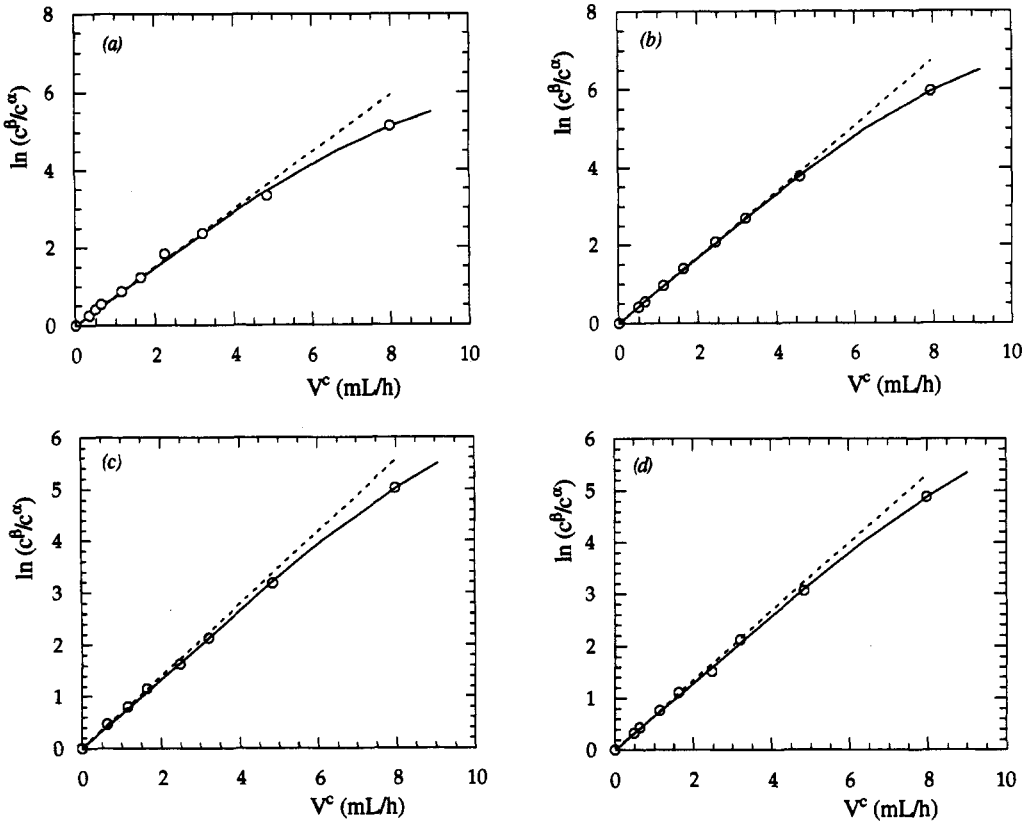

Figure 3. Logarithm of the concentration ratio as a function of convective flow for the following cases: (a) 0.01 M Nacl, Durapore membrane, (b) 0.1 M NaCl, Durapore membrane, (c) 0.01 M KCl, Durapore membrane, and (d) 0.01 M NaCl, MF-Millipore membrane. In each curve, the circles are the experimental points, the continuous line corresponds to the fitting of eq 20 to these points, and the dashed line corresponds to the regression line calculated with the points below 2 mL/h.

number ($\dot{V}^c L/AD$) takes large values (in the range 6–8) when the curves $\ln(c^\beta/c^\alpha)$ vs $\dot{V}^c$ deviate from linear behavior.

The approximation $\bar{c}(x) \approx \bar{c}(0)$ in eq 18 is not strictly necessary, but simplifies the interpretation of the experimental data. Indeed, eqs 1a and 18 show the experimental trends observed in the $\ln(c^\beta/c^\alpha)$ vs $\dot{V}^c$ curve: the (downward) deviation from linear behavior is very small when the electrolyte concentration is high (c^β, $c^\alpha \gg X$, eq 1a), but can be important for low enough electrolyte concentrations ($c^\alpha \approx X$, eq 18).

Finally, following recent studies,[6,7,10] we introduce for X the Freundlich adsorption isotherm:

$$X(0) = k(c^\alpha)^n \quad \text{and} \quad X(L) = k(c^\beta)^n \tag{19}$$

where k and n are two known constants determined in ref 10 from streaming potential measurements for the membranes studied here.

Taking into account all the above assumptions, eq 18 can be written in the form

$$\dot{V}^c = \frac{m_1 q}{1 - m_2 e^q} \tag{20}$$

with

$$m_1 \equiv \frac{AD}{L}, \quad m_2 \equiv \frac{8\gamma\eta D}{RTr_0^2 \bar{c}(L)}, \quad q \equiv \ln \frac{\bar{c}(L)}{\bar{c}(0)} \tag{21}$$

Equation 20 can now be fitted to the experimental points in Figure 2 and Table 1 in order to obtain the values of the parameters m_1 and m_2. This has been done in Figure 3 (in the form of $\ln(c^\beta/c^\alpha)$ vs $\dot{V}^c$ curves) for the following systems: (a) Durapore membrane (nominal pore radius r_0 = 0.05 μm) with c^β = 0.01 M NaCl solution, (b) Durapore membrane (r_0 = 0.05 μm) with c^β = 0.1 M NaCl solution, (c) Durapore membrane (r_0 = 0.05 μm) with c^β = 0.01 M KCl solution, and (d) MF-Millipore membrane (r_0 = 0.11 μm) with c^β = 0.01 M NaCl solution. The streaming potential data in ref 10 provide the values k = 0.569 mM and n = 0.355 for the Durapore membrane and k = 0.113 mM and n = 0.328 for the MF-Millipore membrane; the concentrations c^α and c^β in eq 19 are introduced in millimolar units.

Table 2. Values of Parameters m_1 and m_2 in Eq 21 for Cases a–d

case	m_1 (mL/h)	$100m_2$	case	m_1 (mL/h)	$100m_2$
a	1.43	0.654	c	1.59	0.529
b	1.21	0.088	d	1.58	0.097

The continuous curves in Figure 3 correspond to eq 20 with the values of m_1 and m_2 given in Table 2. The agreement between theory and experiment seems to be reasonable, mainly if we consider the simplicity of the model and the crude nature of many of the assumptions invoked. Since m_1 and m_2 depend explicitly on the experimental characteristics of the system, it is in order now to estimate them from these characteristics. Let us take $A \approx 1$ cm^2, $L \approx 10^{-3}$–10^{-2} cm, and $D \approx 10^{-6}$ cm^2/s. Then, we obtain $m_1 \approx 1$ mL/h, which is in agreement with the values in Table 2. Note that in charged membranes the counterion diffusion coefficient can be considerably smaller than that corresponding to a bulk aqueous solution.[15,17] Indeed, when $r_0 \approx \lambda$, the pore fluid can no longer be considered as a bulk electrolyte solution. On the other hand, the estimate for the value of m_2 yields

(17) Ueda, T.; Kamo, N.; Ishida, N.; Kobatake, Y. *J. Phys. Chem.* **1972**, *76*, 2447. Fair, J. C.; Osterle, J. F. *J. Chem. Phys.* **1971**, *54*, 3307.

$$m_2 \approx \gamma \frac{[8 \times 10^{-3}\ (\mathrm{N\ s})/\mathrm{m}^2](10^{-10}\ \mathrm{m}^2/\mathrm{s})}{[8\ \mathrm{J}/(\mathrm{mol\ K})](300\ \mathrm{K})(10^{-14}\ \mathrm{m}^{-2})(10\ \mathrm{mol}/\mathrm{m}^3)} \approx$$

$$\gamma(3.2 \times 10^{-3}) \approx 10^{-3} \quad (22)$$

where we have considered that $\gamma \lesssim 1$. This value is within the order of magnitude of the results shown in Table 2, which confirms the plausibility of the theory.

We can compare finally the dependence of m_2 on the parameters c^β, r_0, and D for cases a–d above. For this purpose, let us consider the ratios

$$\frac{m_2(\mathrm{a})}{m_2(\mathrm{b})} = \frac{\bar{c}(L)(\mathrm{b})}{\bar{c}(L)(\mathrm{a})} = \begin{cases} 9.5\ (\mathrm{theor}) \\ 7.4\ (\mathrm{exptl}) \end{cases} \quad (23)$$

$$\frac{m_2(\mathrm{a})}{m_2(\mathrm{d})} \approx \left(\frac{r_0(\mathrm{d})}{r_0(\mathrm{a})}\right)^2 = \begin{cases} 4.8\ (\mathrm{theor}) \\ 6.7\ (\mathrm{exptl}) \end{cases} \quad (24)$$

$$\frac{m_2(\mathrm{a})}{m_2(\mathrm{c})} = \frac{D(\mathrm{a})}{D(\mathrm{c})} = \begin{cases} \approx 1\ (\mathrm{theor}) \\ 1.2\ (\mathrm{exptl}) \end{cases} \quad (25)$$

In eqs 23–25 the first number (theor) corresponds to the theoretical expression for m_2 in eq 21 with the values for the experimental conditions in cases a–d, while the second number (exptl) results from the m_2 values in Table 2. We see again that a rather crude model can give a first, very reasonable account of the experimental trends observed.

Discussion

The transport problem dealt with here clearly shows how charged pores affect a classical equation for convective diffusion in porous media. Indeed, the changes observed in the $\ln(c^\beta/c^\alpha)$ vs $\dot{V}^c$ curves with the membrane pore radius, concentrations, etc. can be accounted for on the basis of the charge adsorbed on the pore walls. Also, the absence of experimental deviations from the linear behavior for the case of the scratched membrane seems to speak on behalf of this explanation, though we must recognize that our estimations did not discard definitively an explanation based on the existence of diffusion boundary layers. Let us mention finally that recent streaming potential measurements[10] with the same membranes employed here showed physical trends *similar* to those observed in our case (see Table 3): streaming potential increases when the salt concentration and the pore radius decrease. Although it is clear that these results were obtained under experimental conditions different from those studied here, the fact remains that deviations from the linear behavior in Figure 3 also appear in the above-mentioned range of concentration and pore radius.

Table 3. Slope of the Streaming Potential vs Pressure Drop Curve, $\Delta\phi_{SP}/\Delta p$, for the Same Membranes Considered in Figure 3[10] ($c^\alpha = c^\beta = c$)

	$\Delta\phi_{SP}/\Delta p$ (10^{-9} V/PA)			$\Delta\phi_{SP}/\Delta P$ (10^{-9} V/Pa)	
c (M)	r_0 = 0.05 μm	r_0 = 0.11 μm	c (M)	r_0 = 0.05 μm	r_0 = 0.11 μm
10^{-4}	4500	3920	10^{-2}	64.3	18.2
10^{-3}	753	452	10^{-1}	4.56	2.9

We might speculate now about the possibility of using our approach to estimate the adsorbed charge concentration. Indeed, we have predicted theoretically and demonstrated experimentally that the deviation of the $\ln(c^\beta/c^\alpha)$ vs $\dot{V}^c$ curves from linear behavior give us some information on the *adsorbed charge* in the membrane (this charge is a key parameter in any electrokinetic phenomenon). That is, had we not known the value of this charge "a priori" (e.g., from the streaming potential measurements), we would have been able to estimate it from the fitting of experiment to theory. Unfortunately, it should be emphasized that a rigorous modeling of the problem is more difficult in our case than in the case of the streaming potential. Indeed, *three* physical magnitudes (concentration, pressure, and electric potential) rather than *two* are changing through the membrane in the experimental situation dealt with here.

In conclusion, our study has shown that the adsorbed charge can affect the measurement of the membrane parameter A/L, which can be seen as an independent confirmation of a rather general result:[6-9] ion adsorption on the pore walls of inert, porous membranes can significantly affect the observed transport phenomena, especially in the limit of low bulk concentration and small membrane pore radius.

Acknowledgment. Partial support from the DGICYT under Project No. PB92-0516, Ministry of Education and Science of Spain, for S.M. and J.A.M. is gratefully acknowledged.